International Journal of Science and Research (IJSR)
ISSN (Online): 2319-7064
Index Copernicus Value (2016): 79.57 | Impact Factor (2015): 6.391

CT System Parameters Determination based on Calibration Method

Ling Liu[1], Hao Tang[2], Yuhan Zhou[3], Jun Ye[4]

[1, 2, 4]School of Mathematics and Statistics, Sichuan University of Science and Engineering, Sichuan, China

[3]School of Civil Engineering, Sichuan University of Science and Engineering, Sichuan, China

Abstract: ***Parameter calibration of the installed CT system can reduce the error and improve the imaging quality. Based on the geometric information of the known calibration template, the corresponding absorption rate and the received information, three calibration parameters are obtained by Matlab software programming based on the formulas of Radon transformation and Radon inverse transformation: 180 directions of the X-ray used by the CT system, the detector The distance between units, the center of rotation of the CT system in the square pallet.***

Keywords: CT system; parameter calibration; Radon transformation; Radon inverse transformation

1. Introduction

Computed Tomography(CT), one of the most advanced imaging technologies available today, has become indispensable in the fields of clinical medicine, industry, materials and biology with its advantages of non-contact, non-destructive, high resolution, The important technology. It can take advantage of the sample's ability to absorb radiation energy to tomograph samples of biological tissue and engineered materials without damaging the sample, thereby obtaining structural information inside the sample. CT system[1-5] installation often have errors, thus affecting the imaging quality, which has varying degrees of impact on the application of various fields, the installation of a good calibration of the CT system parameters can reduce the error and thus improve the quality of the imaging, calibration of the CT system parameters Research is of great significance. Based on a typical two-dimensional CT system, the parameters of a CT system were calibrated with the aid of the known sample structure.

Placing a calibration template consisting of two uniform solid media on a square pallet, the geometric information of the template is shown in Figure 1.

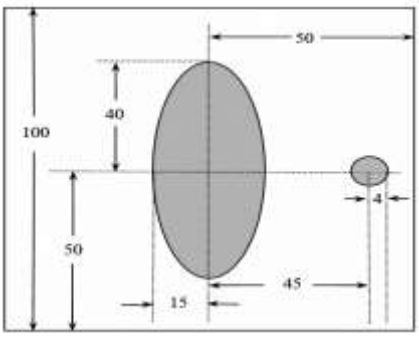

Figure 1: Schematic diagram of the template (unit: mm)

Three calibration parameters can be determined based on the geometry of the calibration template, the absorbance data for each point, and the received message data corresponding to the template: 180 directions of x-rays used by the CT system, between detector elements The distance from the CT system center of rotation in the square tray.

2. Preliminaries

2.1 CT system basic idea

Select a number of ideal X-ray source, uniform arrangement, placed in the opposite side of the X-ray detector to detect the intensity of X-ray radiation emitted by the detector and the detector receives the attenuation of the radiation intensity. Then rotate a small angle to record another set of data at this time.

According to *Beer* theorem:

$$\int_L \mu dl = \ln(I_0 / I)$$

Where μ is the linear attenuation coefficient of the object with respect to the X-ray and L is the path of the X-ray in a certain direction.

In the case of known I_0 and I, $\int_L \mu dl$ can be obtained, and finally according to the distribution of μ images, restore objects.

2.2 Two-dimensional space Radon transformation

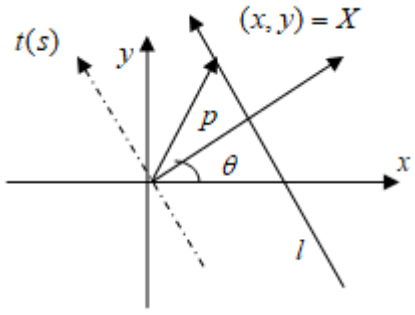

Figure 2: Radon Transform Diagram

Licensed Under Creative Commons Attribution CC BY

If the function $f(x,y)$ is smooth, it means that it is C^{∞}, the expression R^2 on the straight line $l_{p\omega}$ is:

$$p=(x,y)\cdot\omega=x\cos\theta+y\cos\theta$$

Where p is the normal length ($p\geq 0$ as the distance from the origin to the straight line $l_{p\omega}$), θ is the normal vector and the x axis of intersection $(0\leq\theta\leq 2\pi)$, $\omega=(\cos\theta,\sin\theta)$ is the unit vector from the origin to the straight line. The compact set function $f(x,y)$ on R^2 along the linear $l_{p\omega}$ radon transform $Rf(p,\omega)$ is defined as:

$$Rf=\int_{l_{p\xi}} f(x,y)d\sigma=\int_{-\infty}^{+\infty} f(p\cos\theta-s\cos\theta,\ p\sin\theta+s\cos\theta)ds \quad (1)$$

Mark $Rf(p,\theta)=Rf(p,\omega)$, due to:

$$Rf(-p,\omega)=Rf(p,-\omega)$$

The range of (p,θ) variation is consider as:

$$-\infty<p<\infty, 0\leq\theta<\pi$$

Thus, the *Radon* transformation [6-10] is used to calculate the direction of the projection of the image matrix, the projection of the function $f(x,y)$ is a line integral in a certain direction. Let $X=(x,y),\xi=(\cos\theta,\sin\theta)$,then we can give $f(x,y)$ the *Radon* transformation inversion formula:

$$f(x,y)=\frac{-1}{2\pi^2}\int_0^{\pi}d\theta\int_{-\infty}^{+\infty}\frac{1}{p-\xi\cdot X}\frac{\partial Rf}{\partial p}dp \quad (2)$$

Through the above formula can be completed CT imaging system function transformation.

2.3 Simulation Radon transform and Radon inverse transform

Using formula (1) and (2) to do *Radon* transform and *Radon* inverse to the calibration template, Figure 3 and Figure 4 are obtained:

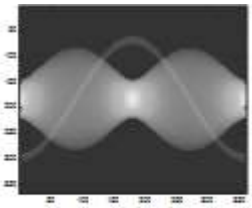

Figure 3: Template after Radon transform diagram

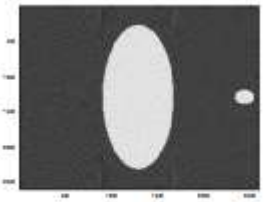

Figure 4: template by Radon inverse transform diagram

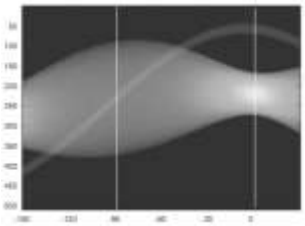

Figure 5: Template to receive information conversion diagram

Figure 4 is consistent with Figure 1, comparing Figure 3 and Figure 5, you can find two pieces of Figure 5 by splicing together very similar to Figure 3, Figure 3 is the simulation of CT scan one week (ie 360 °) to get the absorption rate, and therefore It can be judged that the received information data of this template is the medium absorption information scanned by the detector rotated by 180 °, that is, the total amplitude of rotation is determined, which plays an important role in solving the following model.

3. Mathematic Model

3.1 Directions of X-ray

Use the *Matlab* software to receive the template information of the *Radon* inverse transform, and then according to numerical values from dark to light rules to draw graphics, to restore the template picture, as shown in Figure 6.

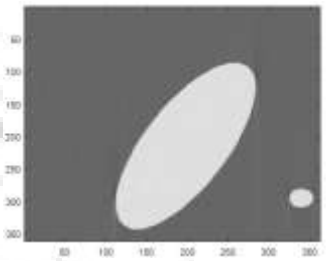

Figure 6: Received information by Radon inverse transform reduction map

Figure 6 shows the position of the medium at the initial detection (ie, non-rotation) of the detector. Combined with the data in the first column of the reception information table of the template, it can be seen that the detector is placed horizontally below and the parallel beams are emitted from top to bottom.

According to the *Matlab* programming solution, the major axis of the vertical elliptical form of the detector beam can be obtained. That is, the major axis of the vertical elliptical form of the detector beam is rotated 62 times when rotating to the vertical direction. The detector beam rotates perpendicular to the minor axis of the elliptical template, that is, rotates 151 times in the horizontal direction.

If the detector is rotated evenly, each rotation angle is:

$$\Delta\theta=\frac{90^{\circ}}{151-62}=1.0112^{\circ}$$

Here, the minor axis of the elliptical template is horizontal 0 °, then the 0th rotation, that is, the initial angle is:

$$90^{\circ}-62\times\Delta\theta=27.3034^{\circ}$$

In summary, the X-ray angle of 180 directions formula is:

$$D=27.3034^{\circ}+C\times\Delta\theta \quad (3)$$

C Is the number of rotations, and

$C=0,1,2,...,179$, when $C=179$, $D=208.3082^{\circ}$

So the range of rotation angle is:

$$[27.3034^{\circ},208.3082^{\circ}]$$

Licensed Under Creative Commons Attribution CC BY

3.2 Detector unit spacing

According to the received data of the template, $N_1(N_1 \geq 289)$ detectors unit is obtained by *Matlab* programmed to pass through the medium perpendicular to the long axis of the ellipse (80mm long from the ellipse shown in Figure 1), so that the detector unit spacing is:

$$d_1 \leq \frac{80}{N_1 - 1} mm \text{ ,which is } d_1 \leq 0.2778mm$$

$N_2(N_2 \geq 108)$ detectors unit will be perpendicular to the short axis of the ellipse (30mm ellipse short axis shown in Figure 1) through the medium, the detector unit spacing:

$$d_2 \leq \frac{30}{N_2 - 1} mm \text{ ,which is } d_2 \leq 0.2804mm$$

$N_3(N_3 \geq 29)$ detectors unit will pass through a small circular medium with a diameter of 8mm, so that the detector unit spacing is:

$$d_3 \leq \frac{8}{N_3 - 1} mm \text{ ,which is } d_3 \leq 0.2857mm$$

Table 1: Detector unit spacing

Corresponding number of detector units *N*	Actual length （mm）	Unit distance *d* （mm）
289	80	0.2778
108	30	0.2804
29	8	0.2857

Detector unit spacing is fixed, the smaller the pitch, the smaller the error, so you can determine the detector unit spacing:

$d = d_1 = 0.2778mm$.

3.3 Rotation center position

Since the error of the rotation center of the CT system deviates from the center of the elliptical medium, the information received by the separation of the small circular medium and the elliptical medium is manually removed. Then, based on the remaining data, the position of the rotation center is obtained by *Matlab* and a square pallet The center is the origin, the horizontal right is the axis, the vertical upward is the rectangular coordinate system of the axis, as shown in Figure7.

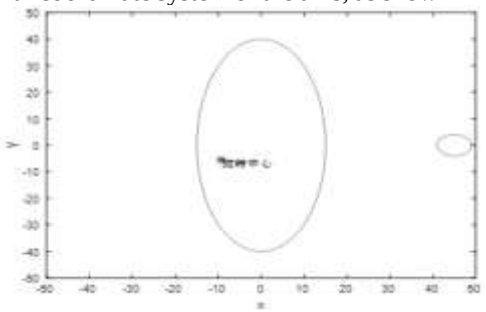

Figure 7: Rotation center position diagram

Theoretically, the center of the ellipse is the origin (rotation center) coordinate $O(0,0)$ of the coordinate system. Due to the installation deviation, the origin coordinate $O'x'y'$ of the scanned coordinate $O'(x_0, y_0)$ is the rotation center and defaults to be the central pixel point of the detector array. The scan coordinate system and the theoretical origin of the coordinate system there is an error l_{x_0} and l_{y_0} .

For the scan coordinate system and the theoretical coordinate system center is not coincident, any point $f(x, y)$ in the scan space, the projection on the detector at different scan angles to follow the following formula [3]:

$$l_x = r \times \cos(\phi - \theta) + l_{x_0}$$

$$l_y = r \times \sin(\phi - \theta) + l_{y_0}$$

The purpose of determining the rotation center is to determine the value of the l_{x_0} and l_{y_0} other information in the formula is redundant, for the formula, the maximum and minimum values of l_x and l_y are:

$$l_{x_{max}} = r + l_{x_0} \quad l_{x_{min}} = -r + l_{x_0}$$

then:

$$l_{x_0} = \frac{l_{x_{max}} + l_{x_{min}}}{2}$$

Empathy:

$$l_{y_0} = \frac{l_{y_{max}} + l_{y_{min}}}{2}$$

Therefore, the projection original data can be analyzed to find the recorded value in the direction of rotation of the theoretical coordinate system, as shown in Figure 8, where the maximum non-zero data interval in this direction is the maximum of non-zero data. Theoretically, the center of the ellipse is located at the origin of the theoretical coordinate system, as shown in Figure 8, the projection points of the two ends of the long axis of the ellipse are $l_{y_{max}}$ and $l_{y_{min}}$ respectively.

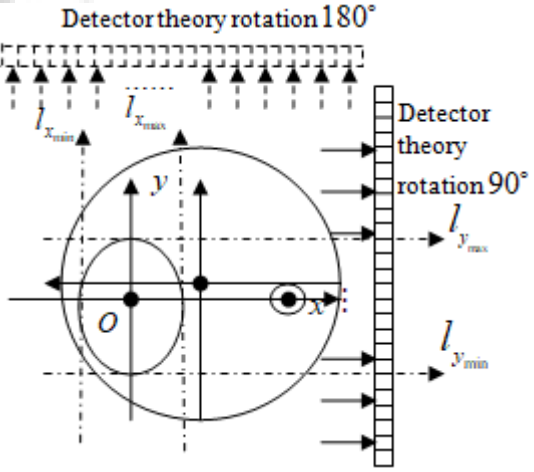

Figure 8: CT theory of rotating scanning probe receiving information schematic

Licensed Under Creative Commons Attribution CC BY

Find the value of the rotation of the theoretical coordinate system 180 times the direction of the record, the direction of the smallest non-zero data interval, that is, non-zero data minimum. As shown in the figure, oval short axis, the first two points of the projection point are $l_{y_{\max}}$ and $l_{y_{min}}$ respectively. Obtained by the above formula:

$$l_{x_0} = \frac{l_{x_{\max}} + l_{x_{\min}}}{2}$$

$$l_{y_0} = \frac{l_{y_{\max}} + l_{y_{\min}}}{2}$$

Based on the given data, the coordinates of the rotation center are calculated by *Matlab* as follows: $(-9.3056, 5.5556)$.

4. Conclusion

In this paper, the calibration of the CT system is completed. The range of 180 directions of the X-ray used by the CT system is: $[27.3034^{\circ}, 208.3082^{\circ}]$,the distance between the detector units is: $0.2778mm$,the position of the center of rotation of the CT system in the square pallet is: $(-9.3056, 5.5556)$.

5. Acknowledgement

This work was supported by the Talent Project of Sichuan University of Science & Engineering (2017RCL23).

Corresponding Author: Jun Ye, yejun@suse.edu.cn

References

[1] Meyer, M., Haubenreisser, H., Schoepf, U. J., Vliegenthart, R., Leidecker, C., Allmendinger, T., & Henzler, T. (2014). Closing in on the K edge: coronary CT angiography at 100, 80, and 70 kV—initial comparison of a second-versus a third-generation dual-source CT system. Radiology, 273(2), 373-382.

[2] Teoh, E. J., McGowan, D. R., Macpherson, R. E., Bradley, K. M., & Gleeson, F. V. (2015). Phantom and clinical evaluation of the Bayesian penalized likelihood reconstruction algorithm Q. Clear on an LYSO PET/CT system. Journal of Nuclear Medicine, 56(9), 1447-1452.

[3] Meyer, M., Haubenreisser, H., Raupach, R., Schmidt, B., Lietzmann, F., Leidecker, C., ... & Henzler, T. (2015). Initial results of a new generation dual source CT system using only an in-plane comb filter for ultra-high resolution temporal bone imaging. European radiology, 25(1), 178-185.

[4] Aloisi, V., Carmignato, S., Schlecht, J., & Ferley, E. (2017, February). Investigation on the effects of X-ray CT system geometrical misalignments on dimensional measurement errors. In 7th conference on industrial computed tomography (iCT) (pp. 7-9).

[5] Ehn, S., Sellerer, T., Muenzel, D., Fingerle, A. A., Kopp, F., Duda, M., ... & Schwaiger, B. J. (2018). Assessment of quantification accuracy and image quality of a full-body dual-layer spectral CT system. Journal of applied clinical medical physics, 19(1), 204-217.

[6] Marzilger, R., Legerlotz, K., Panteli, C., Bohm, S., & Arampatzis, A. (2018). Reliability of a semi-automated algorithm for the vastus lateralis muscle architecture measurement based on ultrasound images. European journal of applied physiology, 118(2), 291-301.

[7] Trnovszký, T., Sýkora, P., & Hudec, R. (2017). Comparison of background subtraction methods on near Infra-Red spectrum video sequences. Procedia engineering, 192, 887-892.

[8] Zakasovskaya, E. V., & Tarasov, V. S. (2018). Optical fiber imaging based tomography reconstruction from limited data.Computer Methods in Applied Mechanics and Engineering,328, 542-553.

[9] Xu, X. L., Xu, S. M., Li, H. Q., & Fan, H. Y. (2017). On the relationship between Collins diffraction integration and quantum tomogram. Optik-International Journal for Light and Electron Optics, 129, 207-211.

[10] Sun, S., & Jiang, Y. (2017). Three-dimensional shipborne inverse synthetic aperture radar imaging based on single receiver. Remote Sensing Letters, 8(4), 320-329.

[11] Zhang, K., Wu, X. L., Yan, J. F., & Cai, J. T. (2017). Electromagnetic holographic sensitivity field of two-phase flow in horizontal wells. Applied Geophysics, 14(1), 40-48.

[12] Li, W., & Wang, J. (2017). A new complex approach towards approximate inverse and generalized Radon transform. Complex Variables and Elliptic Equations, 1-13.

Licensed Under Creative Commons Attribution CC BY